Assessment of membrane fouling and biopolymers in a novel membrane bioreactor-microbial fuel cell hybrid system

Liang Duan[a,b], Yuan Tian[a,b,d], Jian Wei[a,b], Feng Qian[a,b], Jifeng Guo[c],
Yonghui Song[a,b,*], Xiaoling Liu[a,b]

[a]State Key Laboratory of Environmental Criteria and Risk Assessment, Chinese Research Academy of Environmental Sciences,
Dayangfang 8, Anwaibeiyuan, Beijing 100012, China, Tel. +86 18612648868, email: duanliang@craes.org.cn (L. Duan),
Tel. +86 13683127120, email: 1002106371@qq.com (Y. Tian), Tel. +86 10 84915308, email: weijian@craes.org.cn (J. Wei),
Tel. +86 13581643787, email: qianfeng@craes.org.cn (F. Qian), Tel. +86 13811993368, email: songyh@craes.org.cn (Y. Song),
Tel. +86 15011019493, email: liuxl@craes.org.cn (X. Liu)
[b]Department of Urban Water Environmental Research, Chinese Research Academy of Environmental Sciences,
Beijing 100012, China,
[c]School of Environmental Science and Engineering, Key Laboratory of Subsurface Hydrology and Ecology in Arid
Areas of Education Ministry, Chang'an University, Xi'an 710054, China, Tel. +86 13720732593,
email: guojifeng@chd.edu.cn (J. Guo)
[d]College of Water Sciences, Beijing Normal University, Xinjiekou Wai Street 19, Beijing 100875, China

ABSTRACT

A lab-scale hybrid membrane bioreactor-microbial fuel cell system (hMBR) and a single MBR system (sMBR) were compared to investigate the characteristics of membrane fouling and biopolymers. The results indicated that both MBRs had excellent performance in the removal of chemical oxygen demand (COD) and ammonia nitrogen. Although the general compositions of the extracellular polymeric substances (EPS) and the soluble microbial products (SMP) were very similar, the concentrations in the hMBR were lower. An X-ray analysis indicated that Ca, Mg, Si and Fe were prone to accumulate on the membrane surface in the sMBR. An excitation-emission matrix (EEM) analysis showed that more aromatic proteins (I and II) and fewer humic/fulvic acid-like substances were observed in the hMBR. Moreover, almost half of the total components of EPS and SMP were soluble microbial metabolites in the hMBR. In conclusion, the hybrid system could alleviate membrane fouling by influencing the characteristics of the biopolymers.

Keywords: Membrane bioreactor; Microbial fuel cell; Extracellular polymeric substances; Soluble microbial products; Membrane fouling

1. Introduction

Membrane bioreactors (MBRs) are widely applied in wastewater treatment due to their high-quality effluent, small footprint and low sludge production [1–3]. Nonetheless, membrane fouling restricts the further application of MBRs [4,5]. Membrane fouling mainly results from the deposition of suspended solids, the clogging of pores by particles (colloids, flocs, etc.) and the adsorption of colloids and solutes onto and/or into the membrane module [6]. Some studies have suggested that the activated sludge supernatant (colloids, solutes, etc.) plays a more significant role in the membrane fouling compared with biological flocs [7]. The supernatant is mainly composed of soluble microbial products (SMP) containing carbohydrates, nucleic acid substances, proteins, and humic substances [8]. For this reason, SMP have been regarded as the main contributors to membrane fouling [9,10]. In addition, the fouling is affected by the molecular weight (MW) distribution of SMP [11,12].

*Corresponding author.

In recent years, extracellular polymeric substances (EPS) were also identified as a primary foulant in membrane fouling since SMP are regarded as soluble EPS [8]. Meanwhile, membrane fouling has been researched for years without reaching definitive conclusions due to contradictions among the results with respect to the relationship among EPS, SMP and membrane fouling [13]. Furthermore, to alleviate and control membrane fouling, effective approaches have been demonstrated, such as optimizing the operation parameters, enlarging the aeration intensity, developing novel anti-fouling membrane materials and modifying the activated sludge characteristics.

Microbial fuel cells (MFCs) have become a promising technology due to their conversion of organic matter into electrical energy via microorganisms [14,15]. However, in terms of effluent quality and treatment efficiency, the performances were poor due to limited biomass retention when MFCs were used to treat wastewater. Along with the introduction of the self-sustained and carbon neutral systems concepts [16], combined MBR-MFCs have emerged to increase the energy recovery and enhance the wastewater treatment efficiency [17]. Initially, Cha et al. and Zhang et al. tried to combine bioreactors with MFCs (immersed or separated) [18,19]. Subsequently, a stainless mesh was used as both the cathode and the filtering material in a novel bioelectrochemical membrane reactor [20]. This process combined the advantages of MBRs and MFCs, thereby enhancing the performance in terms of the chemical oxygen demand and ammonia nitrogen removal rate (92.4% and 95.6%, respectively). Moreover, MFCs could be used to alter the activated sludge characteristics through weak electrical fields. Although a considerable number of studies have investigated MFCs for wastewater treatment, previous researchers have largely focused on the generation of electricity. The research primarily concerning the modification of activated sludge has been scarcely reported.

Therefore, the overall aims of this work were to evaluate the membrane fouling and to explore the underlying role of EPS and SMP in a MBR-MFC hybrid system. A lab-scale hybrid membrane bioreactor-microbial fuel cell system (hMBR) and a single MBR system (sMBR) were studied in

parallel to compare the membrane fouling in treating synthetic municipal wastewater. In addition, both EPS and SMP were analyzed by three-dimensional excitation-emission matrix (EEM) fluorescence spectroscopy, Fourier transform infrared (FTIR) spectroscopy and molecular weight (MW) distribution analysis to compare their specific compositions.

2. Materials and methods

2.1. Experimental setup and operating conditions

As shown in Fig. 1, two laboratory-scale systems were performed in parallel to treat synthetic municipal wastewater: a hMBR and a sMBR. The hMBR with a two-stage system consisted of an aerobic MBR and a separated MFC. Each MBR has an operating volume of 7 L. The same hollow fiber membrane modules (PVDF, 0.02 m^2, 0.4 μm nominal cutoff, Origin Water Technology Co., Ltd., China) were submerged in the two MBRs, respectively. Microporous aeration discs were also placed at the bottom of the two MBRs, providing a constant air flow of 0.15 N m^3/h to maintain a dissolved oxygen concentration of 3–5 mg/L and mix the suspensions throughout the experiments. The single-chamber air cathode MFC with a non-wet-proofed carbon cloth anode was used in this research. The wet-proofed carbon cloth cathode contained platinum loading of 0.5 mg/cm^2 as a catalyst [21]. The spacing between the anode and cathode was 4 cm. The working volume (8 cm × 8 cm × 4 cm) of the anodic chamber was 0.2 L.

The activated sludge was taken from Beijing Gaobeidian Wastewater Treatment Plant, and the initial mixed liquid suspended solids (MLSS) was 5000 mg/L. The reactors were fed with the same synthetic wastewater (glucose 227 mg/L; starch 227 mg/L; $NaHCO_3$ 254 mg/L; urea 33 mg/L; $MgSO_4 \cdot 7H_2O$ 121 mg/L; $MnCl_2$ 0.13 mg/L; KH_2PO_4 15.4 mg/L; K_2HPO_4 19.6 mg/L; $MgSO_4 \cdot 7H_2O$ 51 mg/L; $FeSO_4 \cdot 7H_2O$ 17.48 mg/L; $ZnCl_2 \cdot 2H_2O$ 0.07 mg/L) for 10 days [22]. Both MBRs were inoculated after the activated sludge properties became stable. For the two MBRs, the hydraulic retention time was 17 h, and the solid retention time was 35 d by discharging 200 mL of sludge once a day. Each MBR was operated in a continu-
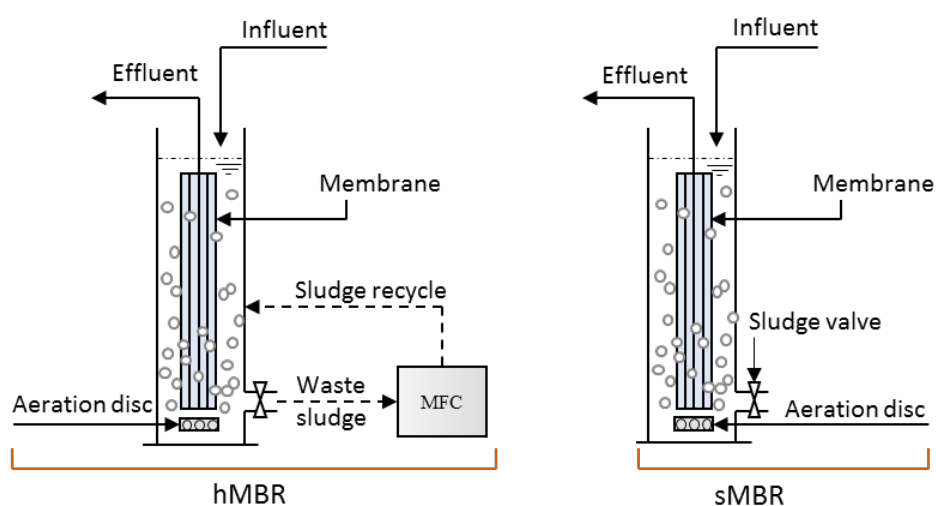
Fig. 1. Schematic diagram of the laboratory-scale reactors.

ous flow mode, and the entire experiment was conducted at room temperature (22 ± 3).

The anodic chamber of the MFC was inoculated with 200 mL of sludge discharged from the hMBR. The sludge was first dumped into a beaker and left to rest for 2 h to get rid of the remnant dissolved oxygen before inoculation. The sludge retention time of MFCs were maintained at 5 d to degrade the EPS and SMP. Totally 5 MFCs were operated alternately and replaced per day during the whole operation. Each MFC was operated at a sequencing batch mode. Total 200 mL sludge was discharged from MFC and circulated to the hMBR each day. Meanwhile, approximately 200 mL of the mixed liquor was discharged from the sMBR for comparison.

2.2. Fouling analysis

2.2.1. TMP measurements

For both MBRs, the flux values were maintained at 20 L/(m²·h). The trans-membrane pressure (TMP) were increased with the reactor running time increased. The TMP was measured by a pressure meter once a day, respectively. When the TMP reached the threshold of the peristaltic pump (40 kPa) during operation, the member module was taken out, washed with tap water, and then immersed in a 0.5% sodium hypochlorite solution for approximately 12 h.

2.2.2. Resistance-in-series model

The different membrane resistances of the filtration analyses were formulated by a series resistance model, as shown in Eq. (1).

$$R_t = R_c + R_f + R_m \tag{1}$$

where R_t is the total membrane resistance (m^{-1}), R_c is the cake layer resistance (m^{-1}), R_f is the internal fouling resistance due to irreversible adsorption and pore blockage (m^{-1}), R_m is the intrinsic membrane resistance (m^{-1}).

According to Eq. (2), R_m could be calculated by measuring the flux and TMP of the new membrane for the filtration of clean water. R_t could be measured from the filtration data before cleaning. After physically cleaning, the fouling layer on membrane surfaces was removed, and all the mem-

branes were placed in tap water to obtain the flux and TMP data and measure $R_f + R_m$. Subsequently, the R_c and R_f could be calculated from Eq. (1).

$$R = \frac{TMP}{\mu J} \tag{2}$$

where R is the filtration resistance (m^{-1}), TMP is the trans-membrane pressure (Pa), J is the permeate flux (m^3/(m²s)) and μ is the permeate viscosity (Pa s).

2.2.3. MFI measurements

The modified fouling index (MFI) could be measured using a batch filtration test (Fig. 2). A stirred ultrafiltration cell 8200 (Millipore, US) was used to investigate the filterability characteristics of the mixed liquor (ML), SMP and suspended solids (SS). The working volume of the cells was 200 mL, and the diameter was 63.5 mm. The effective membrane filtration area was 28.7 cm². The stirring speed of the cells was 120 rpm in this research. First, 150 mL of the MLs of the hMBR and sMBR sludge were centrifuged at 12,000 rpm for 15 min. Then, the supernatants were filtered through filter paper (0.45 μm) to obtain the SMP samples. After that, the pellets were uniformly resuspended in the 150 mL of ultra-pure water, and the resuspended liquors were considered to be the SS samples [23]. All the samples were filtered through an ultrafiltration membrane (normal MW limit 100 kDa, Millipore, US) under a constant pressure of 69 kPa (10 psi) measuring the permeation flux as a function of time [24]. The flux was calculated by weighing the filtered liquor on an electrical balance, which was controlled automatically using Hyper-Terminal software (Hilgraeve, US). In addition, the recording period of balances was 5 s. The plot of t/V versus V (Eq. (3)) was used to determine the MFI (Eq. (4)) [25].

$$\frac{t}{V} = \frac{\mu_W R_m}{\Delta P \Omega} + \frac{\mu_W \alpha C}{2 \Delta P \Omega^2} V \tag{3}$$

$$MFI = \frac{\mu_W \alpha C}{2 \Delta P \Omega^2} \tag{4}$$

where t is the filtration time (s), V is the permeate volume (m^3), μ_W is the dynamic viscosity (Pa s), R_m is the initial mem-
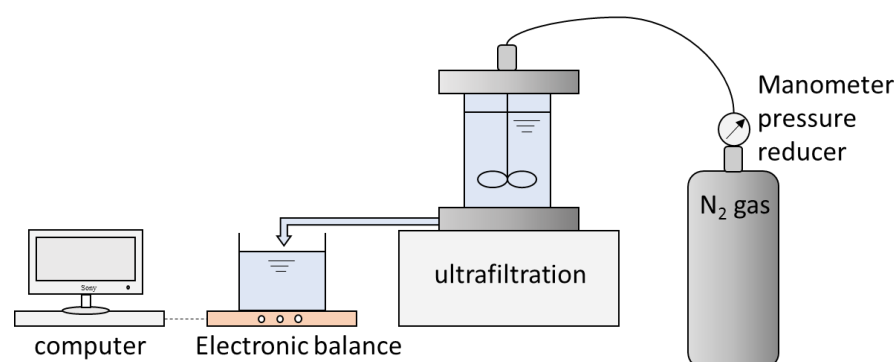
Fig. 2. Schematic diagram of MFI measurement device.

brane resistance (m⁻¹), ΔP is the transmembrane pressure (Pa), Ω is the membrane area (m²), α is the specific resistance (m kg⁻¹) and C is the macromolecule concentration (kg m⁻³).

2.2.4. EDX measurements

Pieces of fouled membranes in the two MBRs were cut from the middle of each module at the end of the experiment. EPS elemental composition analysis of the fouled membrane surface was conducted with energy dispersive X-ray (EDX) spectroscopy (Bruker X Flash Detector 5010, Germany).

2.3. Analytical methods

2.3.1. Analytical methods for water quality parameters

The mixed liquor suspended solids (MLSS) and mixed liquor volatile suspended solids (MLVSS), total chemical oxygen demand (COD), total nitrogen (TN), and ammonia-nitrogen (NH_4-N) concentrations in the influent and effluent of the MBRs were measured according to a standard method [26]. The samples were taken from the two reactors and analyzed every 4 d.

The total extracellular polymeric substances (TEPS), which include the EPS and the SMP, were extracted from the mixed liquor using a cation exchange resin (CER, Sigma-Aldrich, USA). Briefly, 80 mL of activated sludge was centrifuged after the addition of CER to extract the supernatant (12000 rpm, 15 min), which was considered the TEPS. Meanwhile, 80 mL of the sludge samples was centrifuged without the addition of CER, and the resulting supernatant represented the SMP solution [27]. After these two supernatants were filtrated through a filter with a pore size of 0.45 μm, the penetrating fluids were ready for the TEPS and SMP analyses. The concentrations of EPS could be calculated using Eq. (5).

$$TEPS = EPS + SMP \tag{5}$$

The carbohydrates of the TEPS and SMP were determined by the anthrone-sulfuric acid method, and glucose was used as a standard reference [28]. The proteins were measured using a modified Lowry method and bovine serum albumin (BSA) as a standard [29]. The total organic carbon (TOC) was measured by a TOC analyzer (Shimadzu, Japan). DNA was analyzed with a UV-6100 spectrophotometer (Metash, China) at 260 nm, and the concentration was calculated based on Eq. (6).

$$DNA \text{ (mg/mL)} = OD_{260}/0.02 \tag{6}$$

2.3.2. EEM analysis

All the EEM spectra were measured using a fluorescence spectrophotometer (F-7000 FL, Hitachi, Japan). The EEM spectra were collected with subsequent scanning emission spectra from 260 to 550 nm at 5 nm increments by varying the excitation wavelength from 200 to 450 nm at 5 nm increments. The scanning speed was set at 1200 nm/min, and OriginPro 8 software version SR4 (OriginLab Inc., US) was used for processing the EEM data.

2.3.3. FTIR analysis

To obtain information about the major functional groups of the organic substances [30], the TEPS and SMP were placed in a vacuum freeze-dryer (Christ, Germany) for 72 h [24]. Then, the powder samples were measured by FTIR (Equinox 55, Bruker, Germany).

2.3.4. MW analysis

The MW distribution of TEPS and SMP was estimated by filtering the samples through a series of ultrafiltration membranes (Millipore, polyethersulfone, nominal MW cut-off of 1, 10, and 100 kDa) in stirred cell devices 8200 (Millipore, USA). The difference among 1, 10, and 100 kDa was taken as the MWs.

3 Results and discussion

3.1. Degradation performance

The initial MLSS was 5000 mg/L, and the concentrations decreased to 3250 ± 437 mg/L during the whole operation in two MBRs. Both hMBR and sMBR had a satisfied removal efficiency of COD, NH_4-N, and TN during the whole operation (Fig. 3). The two MBRs could remove more than 93% of COD,
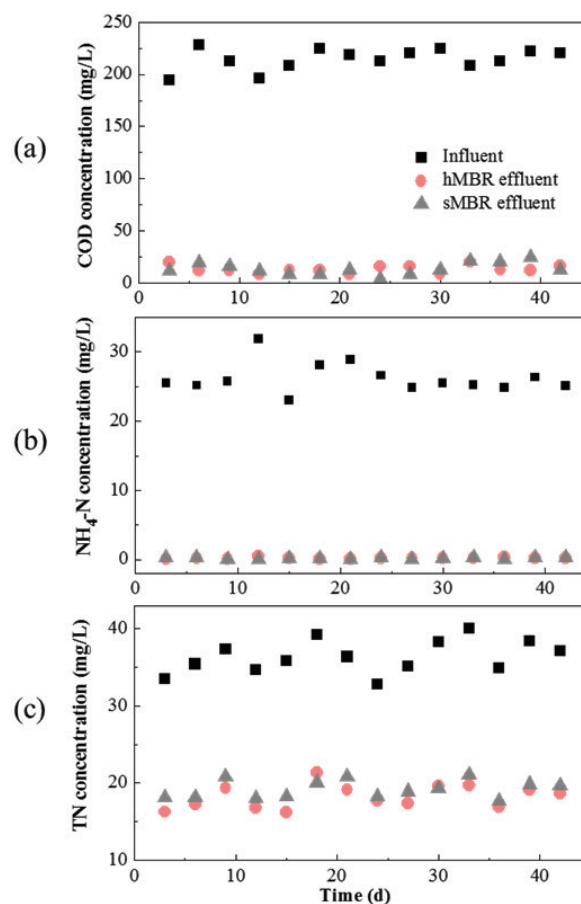
Fig. 3. Temporal variation of COD (a) NH_4-N (b) and TN (c) concentration in hMBR and sMBR.

99% of NH_4-N, and 47% of TN, individually. The average effluent of COD and NH_4-N in the two MBRs was less than 12.6 mg/L and 0.16 mg/L, respectively, which could meet the national discharge standard (COD at 50 mg/L; NH_4-N at 5 mg/L). However, the hMBR increased the average COD, NH_4-N and TN removal efficiencies by approximately 0.31%,

0.12%, and 2.73%, respectively. The results indicated that the MFC was slightly beneficial to the removal of pollutants (Table 1). Su et al. also observed similar results, in which both MBRs could achieve COD and NH_4-N treatment efficiencies of more than 90%, and the combined system (hMBR) behaved slightly better than the sMBR [22]. It was reported that bio-electrochemical systems have positive effects on the degradation of organics and removal of nitrogen and could improve the stability of the anaerobic system [31,32]. Although the removal performance was not significantly different between the reactors, and both reactors had quality discharge levels, the hybrid system can impact the sludge properties, which will lead to an improvement of membrane fouling.

Table 1
Concentrations and removal efficiencies of COD and nitrogen in two MBRs

Items	COD	NH_4-N	TN
Influent wastewater[a] (mg/L)	192.6 ± 36.9	26.86 ± 2.68	36.33 ± 2.12
hMBR effluent[a] (mg/L)	12.0 ± 3.7	0.13 ± 0.12	18.25 ± 1.53
sMBR effluent[a] (mg/L)	12.6 ± 3.9	0.16 ± 0.09	19.24 ± 1.18
hMBR removal efficiency (%)	93.77	99.52	49.77
sMBR removal efficiency (%)	93.46	99.40	47.04

[a]values are given as mean ± standard deviation (number of measurement = 14).

3.2. Fouling characteristics

3.2.1. TMP analysis

As an important parameter, the TMP value was used to evaluate the membrane fouling condition. Fig. 4a illustrates the variations of TMP in two MBRs. The results showed a two-stage process. In Stage 1, the variations of TMP between two MBRs were almost the same in the first 9 d. Then, greater difference of TMP values was noticed in two reactors during operation. This stage was characterized by a gradual fouling stage, which was probably attributed to the accumulation of EPS and the uneven deposition of
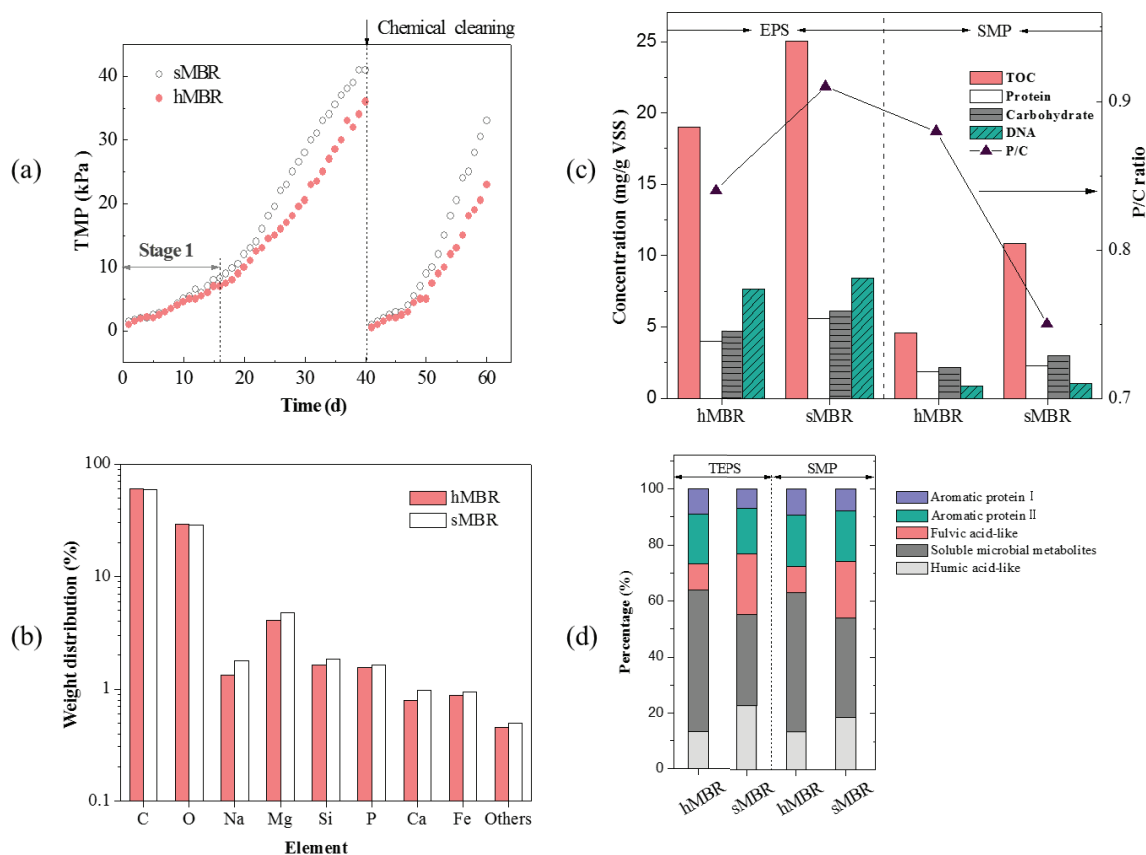
Fig. 4. Analysis of EPS and SMP in two MBRs: (a) Development of TMP as a function of time, (b) EDX analysis of fouled membrane modules, (c) EPS and SMP concentration, (d) FRI distribution.

other biopolymers. In Stage 2, a rapid rise of TMP in both MBRs was observed, which could be due to suspended flocs deposited on the membrane module surface and the gradual change in the structure of the cake layer [33,34]. The TMP in the sMBR was approximately 5–8 kPa higher than in the hMBR after 26 d. The rates of gradual fouling and rapid fouling in the sMBRs were 0.47 kPa/d and 1.51 kPa/d, respectively, which were 14.6% and 17.3% higher than those in the hMBRs (0.40 kPa/d and 1.25 kPa/d). It is worth nothing that the hMBR alleviated the gradual fouling and the rapid fouling by modifying the sludge, which was in accordance with the findings by Su et al. [22]. The TMP reached the threshold of the peristaltic pump (40 kPa) at day 40, and then the membrane module was taken out and cleaned with tap water and a 0.5% sodium hypochlorite solution. It was observed that the fouling speed in both MBRs increased, suggesting that chemical cleaning cannot recover the membrane to the initial stable performance once the membrane module has suffered from fouling. Nonetheless, the growth rate of TMP in the hMBR was slower than in the sMBR after chemical cleaning, which indicated that there were probably certain differences in the sludge characteristics between two MBRs.

3.2.2. Membrane series resistance model

The membrane filtration resistance was used to indirectly characterize the membrane fouling. As shown in Table 2, the internal fouling resistance (R_f) and the cake layer resistance (R_c) were occupied approximately 70% and 27% of the total membrane resistance (R_t) in both MBRs, respectively. Surprisingly, there was a big difference between R_f and R_c in the two MBRs. This was probably due to irreversible adsorption and severe pore blockage. Furthermore, the intrinsic membrane resistance (R_m) was the smallest component of R_t and exhibited a slight difference between the MBRs. The average rates of increase of R_c and R_f in the hMBR were $0.07 \times 10^9 \, \text{m}^{-1} \, \text{d}^{-1}$ and $0.18 \times 10^9 \, \text{m}^{-1} \, \text{d}^{-1}$, respectively, which were 41.7% and 40.0% lower than those in sMBR ($0.12 \times 10^9 \, \text{m}^{-1} \, \text{d}^{-1}$ and $0.3 \times 10^9 \, \text{m}^{-1} \, \text{d}^{-1}$). This result was in accordance with the development of TMP, suggesting that the MFC played an important role in alleviating the membrane fouling.

3.2.3. MFI analysis

The MFI were measured to investigate the filterability characteristics of various components of the sludge, including the mixed liquor (ML), SMP and suspended solids (SS). The MFI value was positively correlated with the membrane fouling potential [35]. As shown in Table 3, the MFI_{ML} of the sMBR was $38 \times 10^3 \, \text{s/L}^2$, which was higher than that of the hMBR and was consistent with the development of the TMP. The MFI of the SMP constituted the main part of the MFI_{ML} in the two MBRs, which occupied 66.7% and 73.7% of the whole MFI in the hMBR and sMBR, respectively. Compared with the MFI_{SMP}, the MFI_{SS} might play a less important role in both MBRs.

3.2.4. EDX analysis

To further investigate the elemental composition of the fouled membrane surface, the EPS of the gel layer were studied with EDX spectroscopy, and the results are shown in Fig. 4b. Most of the elements were comparatively low except for C and O, which had significant influence on the generation of the gel layer even though the quantities of Ca, Mg, Si and Fe were very low [36]. In addition, the multivalent Mg^{2+}, Ca^{2+} and Fe^{3+} cations likely precipitate with and on the surface of the membrane module [37,38]. Once a gel layer was formed, the membrane was difficult to clean with regular aeration. The percentage of these metal ions in the sMBRs was generally higher than in the hMBRs, which was one cause of serious membrane fouling in the sMBRs.

3.3. EPS and SMP characteristics

3.3.1. EPS and SMP concentrations

The concentrations of TOC, proteins, carbohydrates and DNA were analyzed to represent the EPS and SMP, and the average results are shown in Fig. 4c. Compared with the EPS concentration, the SMP concentration was lower in the two reactors. It could be observed that the EPS concentrations (TOC, protein, carbohydrate and DNA) in the sMBR were higher than in the hMBR by approximately 24.0%, 28.5%, 22.6%, and 9.2%, respectively. Meanwhile, the protein/carbohydrate (P/C) ratio for the EPS presented a similar change in both MBRs. Similarly, these SMP concentrations (TOC, protein, carbohydrate and DNA) in the hMBR were lower than 57.5%, 16.2%, 28.1% and 16.0% in the sMBR, respectively. These results provided the evidence that the sMBR underwent more serious membrane fouling. However, one unforeseen result was that the P/C ratio for SMP in the sMBR was lower than that in the hMBR, which was probably a result of modified sludge from the MFC recycling back to the two-stage MBR as a part of the

Table 2
Resistance terms in hMBR and sMBR

Resistance	hMBR		sMBR	
	Values ($10^9 \, \text{m}^{-1}$)	Percentage (%)	Values ($10^9 \, \text{m}^{-1}$)	Percentage (%)
R_t	10.32		17.28	
R_c	2.86	27.7	4.83	27.9
R_f	7.23	70.1	12.18	70.5
R_m	0.23	2.2	0.27	1.6

Table 3
Modified fouling index in hMBR and sMBR

Reactors	MFI ($10^3 \, \text{s/L}^2$)		
	ML	SMP	SS
hMBR	30 ± 5	20 ± 4	6 ± 1
sMBR	38 ± 4	28 ± 2	7 ± 1

[a]values are given as mean ± standard deviation (number of measurement = 3).

influent, which could bring in various SMP into the reactor, thereby changing the P/C relationship. In this current study, SMP were reduced from 17 mg/g VSS to 10 mg/g VSS after employing the hMBR. Su et al. had seen a reduction in EPS and an increase in SMP in an integrated system [22]. The presence of EPS is considered to be the major cause of membrane fouling in the MBRs. Reasonably, a combined MBR–MFC system offers the option of membrane fouling mitigation.

3.3.2. EEM fluorescence spectra

EEM were classified into five regions, which corresponded to tyrosine and tryptophan (Regions I and II), fulvic acid-like (Region III), soluble microbial metabolites (Region IV) and humic acid-like (Region V) [39–41]. To compare the composition of the TEPS and SMP in both MBRs, the EEM spectra were measured, and the results are shown in Fig. 5. The detail fluorescence spectral results, such as the peak location, the maximum fluorescence intensity (FI) and the ratio of the various peak intensities, are listed in Tables 4, 5. It was observed that Peak A at 240/310 nm and Peak B at 275/360 nm of the TEPS were visible in both

MBRs, and those peaks are associated with aromatic protein-like and tryptophan protein-like substances, respectively [39,42,43]. The FIs in the hMBR were much smaller than in the sMBR. Meanwhile, the FIs of peak A and peak B in the hMBR downshifted to 342 and 773, respectively, in reference to the sMBR.

This implies that aromatic protein-like and tryptophan protein-like substances, particularly the latter, might be involved in the membrane fouling. Furthermore, there was a slight difference in the SMP spectrograms in both MBRs,

Table 4
Fluorescence spectral parameters of TEPS in two MBRs

Reactor	Peak A		Peak B		A/B
	Ex/Em	Intensity	Ex/Em	Intensity	
hMBR	240/310	1618	275/360	7327	0.22
sMBR	240/310	1960	275/360	8100	0.24
Existing	Aromatic		Tryptophan		
	protein-like		protein-like		
Substances	Substances		Substances		
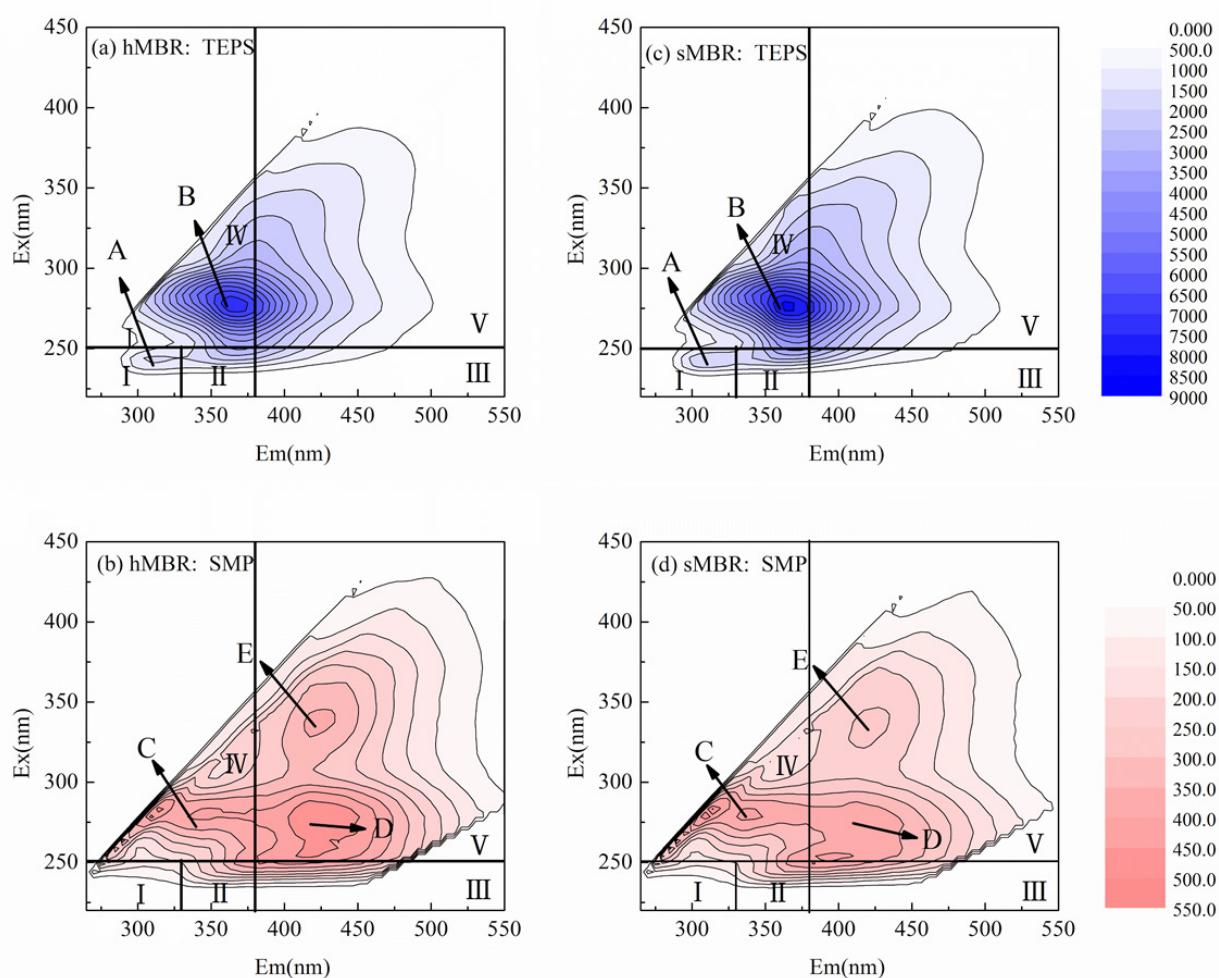
Fig. 5. EEM fluorescence spectra of TEPS and SMP in two MBRs.

Table 5
Fluorescence spectral parameters of SMP in two MBRs

Reactor	Peak C		Peak D		Peak E		C/D	C/E	D/E
	Ex/Em	Intensity	Ex/Em	Intensity	Ex/Em	Intensity			
hMBR	275/340	411.1	275/415	496.2	335/420	360.3	0.82	1.14	1.37
sMBR	275/335	413.8	275/410	391.8	335/420	264.1	1.05	1.56	1.48
Existing	Tryptophan		Humic-like		Visible humic				
Substances	Substances		Substances		Acid-like substances				

and the FIs of those peaks, especially the FI of peak B, were lower than that of TEPS. Table 5 shows that the FI ratios of various peaks are between 0.82 and 1.56, indicating that the FI differences among Peaks C, D, and E are relatively small. It was obvious that the three SMP peaks were found at 275/335–340 nm (Peak C), 275/410–415 nm (Peak D) and 335/420 nm (Peak E) in both MBRs, which were associated with tryptophan, humic-like and visible humic acid-like substances, respectively [39,44]. However, it was interesting that the FI ratios (A/B, C/D, C/E and D/E) in the hMBR were lower than in the sMBR, which indicated less membrane fouling in hMBR.

Fluorescence regional integration (FRI) was used as a semi-quantitative technique to further analyze the EEM spectra. The FRI results showed a conspicuously different distribution of the five regions (Fig. 4d). The aromatic proteins (regions I and II) constituted a quarter of the total substances for both EPS and SMP in the two MBRs. It was obvious that almost half of the total components of EPS and SMP were soluble microbial metabolites in the hMBR but comprised less than 36% in the sMBR. Interestingly, more aromatic proteins (I and II) and fewer humic/fulvic acid-like substances were observed in the hMBR. However, aromatic protein-like substances were thought to be more easily biodegraded by microorganisms [44]. These substances were closely correlated with the formation and degradation of organic matter and played a key role in the membrane fouling process.

3.3.3. FTIR spectroscopy

FTIR spectroscopy was used to investigate the main functional groups of the TEPS and SMP. As shown in Fig. 6, the spectrum revealed a broad region of adsorption at approximately 3400 cm^{-1}, which is attributed to the stretching vibration of the O-H bond in hydroxyl functional groups [45,46]. The intense bands at approximately 1350 cm^{-1} and 1125 cm^{-1} indicate that C-N bonds, polysaccharides, and polysaccharide-like substances were abundant in the SMP of the two MBRs [47]. Furthermore, the main absorption bands of the TEPS were approximately 2540 cm^{-1} (aliphatic C-H stretching), 1625 cm^{-1} (C=O stretching of amide I), 1350 cm^{-1} (C-N stretching) and 1125 cm^{-1} [48]. The sharp peaks at 600–800 cm^{-1} (part of fingerprint region) could be ascribed to aromatic compounds, which are likely humic substances [49]. Briefly, the main components of the TEPS and SMP in both MBRs were proteins, humic substances, polysaccharides and polysaccharide-like substances.
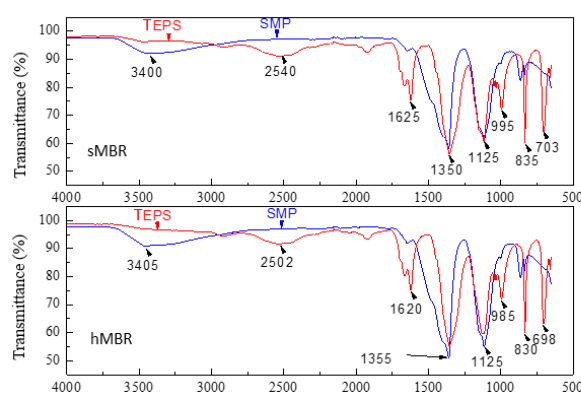
Fig. 6. FTIR spectrum of TEPS and SMP in sMBR (top) and hMBR (bottom).

3.3.4. MW distribution

The MW distribution presented similar distribution between the EPS and SMP in both reactors (Fig. 7). The major components of the EPS were composed of large MW components (> 100 kDa) and low MW components (<1 kDa). Approximately 50.9% and 64.9% of the carbohydrates were categorized as large MW components (>100 kDa) in the hMBR and sMBR, respectively, and approximately 67.8% and 74.3% of the DNA molecules were less than 1 kDa. Compared with the sMBR, the hMBR enhanced the degradation of carbohydrates with MWs larger than 10 kDa. However, other substances (proteins, carbohydrates, and DNA) at medium MW components (1–100 kDa) were present in lower amounts (approximately 9.1–13.3%) except proteins with 10–100 kDa. In terms of SMP, the low MW components (<1 kDa) were the major component (54.3–91.5%) of all the substances, and the percentages were higher in the sMBR than in the hMBR. The low MW components (<1 kDa) were more likely to deposit and clog the membrane pores, thereby accelerating the formation of pore fouling layer. It features a very dense structure and has a very low permeability, resulting in the highest specific biopolymer resistance [35,50]. Statistically, the TOC (>100 kDa), DNA (>100 kDa) and proteins (1–100 kDa) in the sMBR were, on average, slightly higher than in the hMBR. These results further confirm that the sMBR is susceptible to severe membrane fouling, and the hMBR could alleviate the membrane module fouling by modifying the sludge characteristics.
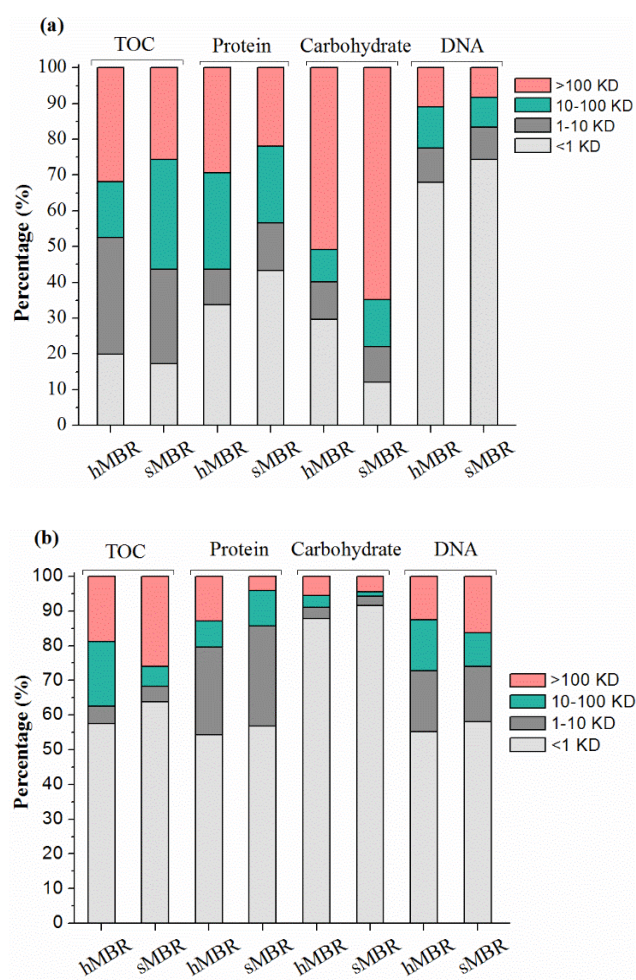
Fig. 7. MW distribution of (a) EPS and SMP (b) in two MBRs.

4. Conclusions

Both MBRs demonstrated good performance in the removal of COD and ammonium. The MFC played a key role in the modification of sludge, thereby alleviating membrane fouling. The membrane filtration resistance model indicated that the average rates of increase of R_c and R_f in the hMBR were lower than in the sMBR. The MFI of the SMP was a main component of the MFI_{ML} in the two MBRs, and the SMP played a more important role in the sMBR. The EDX analysis indicated that Ca, Mg, Si and Fe were more likely to accumulate on the membrane surface in the sMBR. The EEM analysis showed that fewer aromatic proteins (I and II), soluble microbial metabolites and more humic/fulvic acid-like substances were observed in the sMBR. Additionally, more low-MW components (< 1 kDa) of SMP were observed in the sMBR.

Acknowledgments

References

[1] S.I. Khan, I. Hashmi, S.J. Khan, R. Henderson, Performance and optimization of lab-scale membrane bioreactors for synthetic municipal wastewater, Desal. Water Treat., 57 (2016) 29193–29200.

[2] B.J.L. Yeo, S.W. Goh, J.S. Zhang, A.G. Livingston, A.G. Fane, Novel MBRs for the removal of organic priority pollutants from industrial wastewaters: a review, J. Chem. Technol. Biot., 90 (2015) 1949–1967.

[3] H.Y. Ng, S.W. Hermanowicz, Membrane bioreactor operation at short solids retention times: performance and biomass characteristics, Water Res., 39 (2005) 981–992.

[4] F.G. Meng, S.R. Chae, A. Drews, M. Kraume, H.S. Shin, F.L. Yang, Recent advances in membrane bioreactors (MBRs): Membrane fouling and membrane material, Water Res., 43 (2009) 1489–1512.

[5] I.S. Chang, P. Le Clech, B. Jefferson, S. Judd, Membrane fouling in membrane bioreactors for wastewater treatment, J. Environ. Eng.-Asce, 128 (2002) 1018–1029.

[6] P. Le-Clech, V. Chen, T.A.G. Fane, Fouling in membrane bioreactors used in wastewater treatment, J. Membr. Sci., 284 (2006) 17–53.

[7] E. Bouhabila, R. Ben Aim, H. Buisson, Fouling characterisation in membrane bioreactors, Sep. Purif. Technol., 22–3 (2001) 123–132.

[8] S. Liang, C. Liu, L.F. Song, Soluble microbial products in membrane bioreactor operation: Behaviors, characteristics, and fouling potential, Water Res., 41 (2007) 95–101.

[9] S. Rosenberger, C. Laabs, B. Lesjean, R. Gnirss, G. Amy, M. Jekel, J.C. Schrotter, Impact of colloidal and soluble organic material on membrane performance in membrane bioreactors for municipal wastewater treatment, Water Res., 40 (2006) 710–720.

[10] M.E.H. Rojas, R. Van Kaam, S. Schetrite, C. Albasi, Role and variations of supernatant compounds in submerged membrane bioreactor fouling, Desalination, 179 (2005) 95–107.

[11] S. Arabi, G. Nakhla, Impact of molecular weight distribution of soluble microbial products on fouling in membrane bioreactors, Sep. Purif. Technol., 73 (2010) 391–396.

[12] T. Jiang, M.D. Kennedy, V. De Schepper, S.N. Nam, I. Nopens, P.A. Vanrolleghem, G. Amy, Characterization of soluble microbial products and their fouling impacts in membrane bioreactors, Environ. Sci. Technol., 44 (2010) 6642–6648.

[13] C. Jarusutthirak, G. Amy, Role of soluble microbial products (SMP) in membrane fouling and flux decline, Environ. Sci. Technol., 40 (2006) 969–974.

[14] H. Liu, R. Ramnarayanan, B.E. Logan, Production of electricity during wastewater treatment using a single chamber microbial fuel cell, Environ. Sci. Technol., 38 (2004) 2281–2285.

[15] G.C. Gil, I.S. Chang, B.H. Kim, M. Kim, J.K. Jang, H.S. Park, H.J. Kim, Operational parameters affecting the performance of a mediator-less microbial fuel cell, Biosens. Bioelectron., 18 (2003) 327–334.

[16] X. Guo, Y.L. Zhan, C.M. Chen, S.X. Sun, L.J. Zhao, S.H. Guo, Simultaneous bioelectricity generation and biodegradability improvement of refinery wastewater using microbial fuel cell technology, Desal. Water Treat., 53 (2015) 2740–2745.

[17] W. Miran, K. Rasool, M. Nawaz, A. Kadam, S. Shin, J. Heo, J. Jang, D.S. Lee, Simultaneous electricity production and Direct Red 80 degradation using a dual chamber microbial fuel cell, Desal. Water Treat., 57 (2016) 9051–9059.

[18] B.G. Zhang, H.Z. Zhao, S.G. Zhou, C.H. Shi, C. Wang, J.R. Ni, A novel UASB-MFC-BAF integrated system for high strength molasses wastewater treatment and bioelectricity generation, Bioresour. Technol., 100 (2009) 5687–5693.

[19] J. Cha, S. Choi, H. Yu, H. Kim, C. Kim, Directly applicable microbial fuel cells in aeration tank for wastewater treatment, Bioelectrochemistry, 78 (2010) 72–79.

[20] Y.K. Wang, G.P. Sheng, W.W. Li, Y.X. Huang, Y.Y. Yu, R.J. Zeng, H.Q. Yu, Development of a novel bioelectrochemical membrane reactor for wastewater treatment, Environ. Sci. Technol., 45 (2011) 9256–9261.

[21] S. Cheng, H. Liu, B.E. Logan, Power densities using different cathode catalysts (Pt and CoTMPP) and polymer binders (Nafion and PTFE) in single chamber microbial fuel cells, Environ. Sci. Technol., 40 (2006) 364–369.

[22] X.Y. Su, Y. Tian, Z.C. Sun, Y.B. Lu, Z.P. Li, Performance of a combined system of microbial fuel cell and membrane bioreactor: Wastewater treatment, sludge reduction, energy recovery and membrane fouling, Biosens. Bioelectron., 49 (2013) 92–98.

[23] M.L. Pellegrin, K. Min, J. Diamond, M.E. Sadler, A.D. Greiner, K. Zhang, J. Aguinaldo, S. Arabi, M. Liu, M.S. Burbano, L.P. Padhye, F. Kent, R. McCandless, Membrane processes, Water Environ. Res., 86 (2014) 1101–1197.

[24] L. Duan, S. Li, L. Han, Y.H. Song, B.H. Zhou, J. Zhang, Comparison between moving bed-membrane bioreactor and conventional membrane bioreactor systems. Part I: membrane fouling, Environ. Earth Sci., 73 (2015) 4881–4890.

[25] S. Ognier, C. Wisniewski, A. Grasmick, Influence of macromolecule adsorption during filtration of a membrane bioreactor mixed liquor suspension, J. Membr. Sci., 209 (2002) 27–37.

[26] O.E. Albertson, Changes in the biochemical oxygen demand procedure in the 21st edition of standard methods for the examination of water and wastewater, Water Environ. Res., 79 (2007) 453–455.

[27] B. Frolund, R. Palmgren, K. Keiding, P.H. Nielsen, Extraction of extracellular polymers from activated sludge using a cation exchange resin, Water Res., 30 (1996) 1749–1758.

[28] D.L. Morris, Quantitative determination of carbohydrates with dreywoods anthrone reagent, Science, 107 (1948) 254–255.

[29] O.H. Lowry, N.J. Rosebrough, A.L. Farr, R.J. Randall, Protein measurement with the folin phenol reagent, J. Biol. Chem., 193 (1951) 265–275.

[30] T. Maruyama, S. Katoh, M. Nakajima, H. Nabetani, T.P. Abbott, A. Shono, K. Satoh, FT-IR analysis of BSA fouled on ultrafiltration and microfiltration membranes, J. Membr. Sci., 192 (2001) 201–207.

[31] W.Z. Liu, Z.W. He, C.X. Yang, A.J. Zhou, Z.C. Guo, B. Liang, C. Varrone, A.J. Wang, Microbial network for waste activated sludge cascade utilization in an integrated system of microbial electrolysis and anaerobic fermentation, Biotechnol. Biofuels, 9 (2016).

[32] Z.C. Guo, W.Z. Liu, C.X. Yang, L. Gao, S. Thangavel, L. Wang, Z.W. He, W.W. Cai, A.J. Wang, Computational and experimental analysis of organic degradation positively regulated by bioelectrochemistry in an anaerobic bioreactor system, Water Res., 125 (2017) 170–179.

[33] B.D. Cho, A.G. Fane, Fouling transients in nominally sub-critical flux operation of a membrane bioreactor, J. Membr. Sci., 209 (2002) 391–403.

[34] J. Zhang, H.C. Chua, J. Zhou, A.G. Fane, Factors affecting the membrane performance in submerged membrane bioreactors, J. Membr. Sci., 284 (2006) 54–66.

[35] L. Duan, Z.Y. Tian, Y.H. Song, W. Jiang, Y. Tian, S. Li, Influence of solids retention time on membrane fouling: characterization of extracellular polymeric substances and soluble microbial products, Biofouling, 31 (2015) 181–191.

[36] Z.W. Wang, Z.C. Wu, X. Yin, L.M. Tian, Membrane fouling in a submerged membrane bioreactor (MBR) under sub-critical flux operation: Membrane foulant and gel layer characterization, J. Membr. Sci., 325 (2008) 238–244.

[37] X.X. Yan, M.R. Bilad, R. Gerards, L. Vriens, A. Piasecka, I.F.J. Vankelecom, Comparison of MBR performance and membrane cleaning in a single-stage activated sludge system and a two-stage anaerobic/aerobic (A/A) system for treating synthetic molasses wastewater, J. Membr. Sci., 394 (2012) 49–56.

[38] A. Seidel, M. Elimelech, Coupling between chemical and physical interactions in natural organic matter (NOM) fouling of nanofiltration membranes: implications for fouling control, J. Membr. Sci., 203 (2002) 245–255.

[39] W. Chen, P. Westerhoff, J.A. Leenheer, K. Booksh, Fluorescence excitation - Emission matrix regional integration to quantify spectra for dissolved organic matter, Environ. Sci. Technol., 37 (2003) 5701–5710.

[40] M. Bilal, A. Jaffrezic, Y. Dudal, C. Le Guillou, S. Menasseri, C. Walter, Discrimination of farm waste contamination by fluorescence spectroscopy coupled with multivariate analysis during a biodegradation study, J. Agr. Food Chem., 58 (2010) 3093–3100.

[41] S.R. Ahmad, D.M. Reynolds, Monitoring of water quality using fluorescence technique: Prospect of on-line process control, Water Res., 33 (1999) 2069–2074.

[42] G.P. Sheng, H.Q. Yu, Characterization of extracellular polymeric substances of aerobic and anaerobic sludge using three-dimensional excitation and emission matrix fluorescence spectroscopy, Water Res., 40 (2006) 1233–1239.

[43] A. Baker, Fluorescence excitation-emission matrix characterization of some sewage-impacted rivers, Environ. Sci. Technol., 35 (2001) 948–953.

[44] G.C. Huang, F.G. Meng, X. Zheng, Y. Wang, Z.G. Wang, H.J. Liu, M. Jekel, Biodegradation behavior of natural organic matter (NOM) in a biological aerated filter (BAF) as a pretreatment for ultrafiltration (UF) of river water, Appl. Microbiol. Biot., 90 (2011) 1795–1803.

[45] H.C. Xu, G.H. Yu, H.L. Jiang, Investigation on extracellular polymeric substances from mucilaginous cyanobacterial blooms in eutrophic freshwater lakes, Chemosphere, 93 (2013) 75–81.

[46] Y. An, Z.W. Wang, Z.C. Wu, D.H. Yang, Q. Zhou, Characterization of membrane foulants in an anaerobic non-woven fabric membrane bioreactor for municipal wastewater treatment, Chem. Eng. J., 155 (2009) 709–715.

[47] F.G. Meng, H.M. Zhang, F.L. Yang, L.F. Liu, Characterization of cake layer in submerged membrane bioreactor, Environ. Sci. Technol., 41 (2007) 4065–4070.

[48] H.F. Zhang, Impact of soluble microbial products and extracellular polymeric substances on filtration resistance in a membrane bioreactor, Environ. Sci. Technol., 26 (2009) 1115–1122.

[49] T. Tran, B. Bolto, S. Gray, M. Hoang, E. Ostarcevic, An autopsy study of a fouled reverse osmosis membrane element used in a brackish water treatment plant, Water Res., 41 (2007) 3915–3923.

[50] U. Metzger, P. Le-Clech, R.M. Stuetz, F.H. Frimmel, V. Chen, Characterisation of polymeric fouling in membrane bioreactors and the effect of different filtration modes, J. Membr. Sci., 301 (2007) 180–189.